Composite processing and study of properties for polypropylene EPD60R/modified nanoclay Cloisite® 15A

Ali Farahani[1], Arsalan Parvareh[2,*], Mostafa Keshavarz Moraveji[3], Davood Soudbar[4]

[1] Department of Chemical Engineering Borujerd Branch, Islamic Azad University, Borujerd, Iran

[2] Chemical Engineering & Petrol Faculty, Razi University, Kermanshah, Iran

[3] Chemical Engineering Department, Amirkabir University of Technology, Tehran, Iran

[4] Shazand Petrochemical Company, Research and Development Unit, Arak, Iran

HIGHLIGHTS

- A melt compounding method was used to combine polypropylene grid PP60R and nanoclay Cloisite® 15A.

- Submission point of a nanocomposite with 2 and 5% of nanoclay showed an increase of 23 and 29% compared to PP.

- The mechanical properties of strength and modulus of the nanocomposites increases with the addition of nanoclay.

- According to the increase in some mechanical properties, increasing the amount of nanoclay added to the nanocomposite reduces the elongation at break and at yield and submission points.

GRAPHICAL ABSTRACT
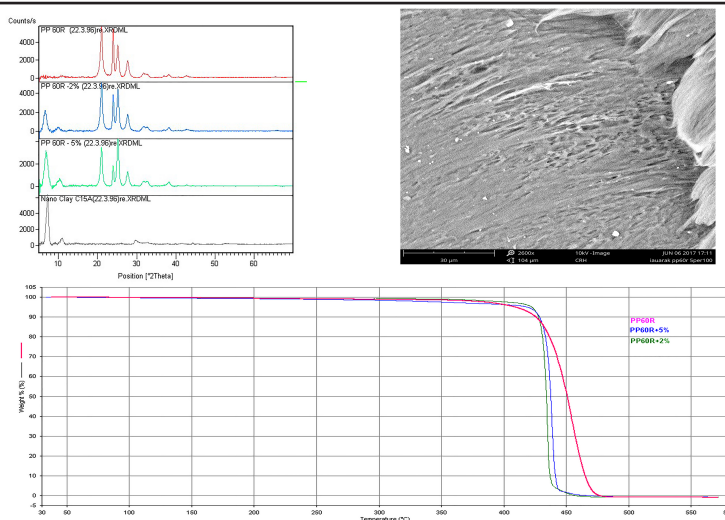
ARTICLE INFO

ABSTRACT

The effects of adding nanoclay to improve the thermal and mechanical properties of polypropylene (PP) copolymers grade (EPD60R) used in the pipe industry were investigated. To improve the dispersion of the nanoclay in the polymeric matrix, a 30 wt% of nanoclay master batch was first prepared by mixing PP matrix maleic anhydride PP oligomer (PP-*g*-MA) and Cloisite® 15A (C15A) nanoclay. The prepared master batch was used to produce nanocomposites with 2 and 5 wt% nanoclay. The nanocomposites were analyzed by XRD (X-ray diffraction), SEM (Scanning electron microscopy), DSC (Differential scanning calorimetry), TGA (Thermogravimetric analysis), and other mechanical tests. The XRD and SEM results indicated the occurrence of an intercalated layer structure in the nanocomposites. Thermal properties of the nanocomposites were investigated using DSC and TGA tests. The crystallinity of the 2 wt% nanoclay was improved by about 59.23% in the nanoclay reinforced samples. As the content of nanoclay increased, the composite exhibited higher thermal degradation temperature. Performing a limiting oxygen index (LOI) test on the samples showed that the addition of nanoclay to the EPD60R matrix increased the flame retardancy by 12.58%. The tensile modulus of the nanocomposites was improved compared to the pure polymer, while the elongation at break and at yield showed a reduction. To investigate the nanocomposite in pipe application, a pipe (external diameter 110.8 and thickness 3.65 mm) was manufactured in a special tube extruder machine with 2 wt% of C15A. Tests of the tube's physical and mechanical properties indicated that its ring stiffness increased by 25% compared to the pure PP.

1. Introduction

Polypropylene/carbon fiber nanocomposites are introducing an attractive new field for applications of polymeric materials in industry. Addition of a small amount of nanoparticles to the polymer matrix can considerably improve the thermal, physical, and mechanical properties of these materials [1,2]. Toyonaga *et al.* prepared a PP nanocomposite of zinc oxide nanoparticles [3]. In this paper, a series of PP-grafted silica nanoparticles (PP-*g*-SiO$_2$) were synthesized by varying the number of grafted chains per silica particle, and influence of the number and molecular weight of grafted chins were studied on the physical properties of PP/PP-*g*-SiO$_2$ nanocomposites. One method to improve the PP pipe performance is the addition of nanoparticles. The PP/nanoclay nanocomposites are introducing an attractive new field for applications of polymeric materials in industry. Adding a small amount of nanoparticles to the polymer matrix can improve its properties [4]. Buasri *et al.* examined the effects of sodium stearate-modified calcium carbonate nanoparticles on the PP matrix [5]. They prepared nanocomposites by twin screw extruder and injection molding machine. The results showed that sodium stearate attached to the surface of CaCO$_3$ nanoparticles with a chemical bond. The other important effects of nanoclay on PP properties is the improvement of flame retardancy. This mechanism is attributed to the formation of carbons silicate on the surface of the polymer, which acts as protection against heat and mass transfer. The formation of protective silicate layers plays a significant role in inhibiting the thermo-oxidative degradation of the polymer [6,7]. A uniform distribution of nanofiller in polymer matrix improves the properties of PP. Maleic anhydride was grafted (PP-*g*-MA) with a variety of molecular weights and acid contents to enhance the interaction with the nanoclay [8-10]. Plaza and Masmira prepared a PP nanocomposite with 1, 3, and 5 wt% using a modified spherical silica nanoparticle [11,12]. Mechanical tests indicated that adding about 5 wt% of spherical silica nanoparticle to the PP matrix can increase the elastic modulus up to 1.6% compared to pure PP. Dabrowska and Zheng prepared a nanocomposite based on PP AR-805 using silica as the nanoparticle [13,14]. The SEM test revealed that the nanoclay had been dispersed uniformly in the polymer matrix, and the thermal and mechanical properties of the nanocomposite were improved. Mirjalili *et al.* reported the preparation of a nanocomposite containing PP and nano α-Al$_2$O$_3$ particles using a Haake internal mixer [15]. Mechanical tests showed that mechanical properties of the composite were enhanced by the addition of nano α-Al$_2$O$_3$ particles and dispersant agent to the polymer. The results of flexural analysis indicated that the maximum values of flexural strength and flexural modulus for nanocomposite were enhanced in the presence of dispersant agent. Transmission and scanning electron microscopic observations of the nanocomposites also showed that fracture surface became rougher by increasing the content of filler loading.

This study aims to resolve these problems by adding nanoclay to PP in pilot and laboratory conditions. Therefore, the first master batch with 30 wt% nanoclay, PP matrix and compatibilizer (PP-*g*-MA) was prepared. Then PP composites with 2 and 5 wt% nanoclay concentrations were produced using a research compounder. The scope of this investigation was expanded to include thermal, mechanical and other properties. To do this, we tried to enhance ring stiffness property by adding nanoclay because nanoclay has a high surface-to-volume ratio, resulting in a lot of interactions, which increases the properties of PP. Manufactured under the license of the Basell company, EPD60R is used in pipe application. Some of the problems industries have with this grade of pipe is inclusive low ring stiffness, flame retardancy and performance. In this study, we investigated this grade of C15A for the first time concentrating on improving its industrial application at the Arak petrochemical company.

2. Experimental

2.1. Materials and methods

EPD60R copolymer was provided by the Shazand Petrochemical company. The nanoclay was purchased from the Zhesiang Fenchong company (China) under the name DK4. The montmorillonite is a hydrophobic natural clay which was modified by alkyl ammonium salts to find organophilic property. The characteristics of the nanoclay, EPD60R, and compatibilizer (PP-*g*-MA) are represented in Tables 1 and 2, respectively.

The composites were prepared with the equipment compounder BAU TEK L$_{40}$/D$_{19}$. The microstructure of

Table 1. Closite 15A® nanoclay characteristics.

Manufacturer	Fanchong
x-Ray d_{001} (A)	36
Specific Gravity (g.cm^{-3})	1.7
Moisture (%)	3
Montmorillonite (%)	98
2θ	7.19

Table 2. EPD60R and compatibilizer (PP-*g*-MA) characteristics.

Batch No.	Manufacturer	MFI g.10min^{-1} (5kg/230 ºC)	D (g.cm^{-3})
EPD60R	Shazand Petrochemical Co.	0.9	0.904
PP-*g*-MA	Aria Polymer	17	0.913

the EPD60R/nanoclay was analyzed with a machine model PROX, TGA analysis were done using PERKIN ELMER, XRD tests were done using a Philips X˙pert diffractometer, DSC analysis were carried out on an PERKIN ELMER DIAMOND, tensile tests were performed by the INESTRON model 1441, and the flexural strength tests were carried out using a WIKI PG. The ring stiffness test was carried out using the machine model SRST.

2.2. Preparation of PP/nanoclay nanocomposites

The master batch was used in the preparation of the nanocomposites for environmental considerations and a more efficient dispersion of nanoclay in EPD60R.

2.2.1. Master batch

Master batch was prepared using a melting mix method with 30 wt% nanoclay, 5 wt% (PP-*g*-MA), and 65 wt% based polymer in a compounder at 180 °C and 100 rpm.

2.2.2. Nanocomposite preparation

The PP nanocomposites were prepared from the master batch using a direct melting mix method with 2 and 5 wt% nanoclay, PP, and PP-*g*-MA in a compounder at 180 °C and 100 rpm for 8 min. At each stage, 500 g of the specimen at various concentrations was prepared. Table 3 indicates the weight percent of the prepared nanocomposites.

Table 3. Percentage of materials used for the preparation of the nanocomposites of EPD60R.

Batch No.	EPD60R (wt%)	PP-g-MA (wt%)	C15A (wt%)
EPD60R$_1$	100	0	0
EPD60R$_2$	93	5	2
EPD60R$_3$	90	5	5

2.3. Characterization

2.3.1. SEM

The SEM was used to ensure the steady dispersion of the modified nanoclay in the polymer matrix, with a magnification range of up to 50000 times and 25 kV.

2.3.2. XRD

The XRD method has been used to investigate the crystalline structure of the nanoclay, nanocomposite, and the distribution of polymeric chains. A shift towards lower angles in the XRD peak suggests an increase in interlayer spacing within the clay layers, which is referred to as intercalation. This test is based on 2θ of 10° to 70° with a 40 kV, 30 mA generators at 25 °C.

2.3.3. DSC

The DSC analysis was performed at temperatures from 25 to 230 °C at a heating rate of 10 °C.min^{-1} increment, after which the samples stayed at 230 °C for 5 minute, then were cooled from 230 to 25 °C and reheated from 25 to 230 °C in the same increments.

2.3.4. TGA

The thermal behavior of the samples was studied by thermogravimetric analyzed under nitrogen atmosphere with a flow rate of 20 mL/min and a scan heating rate of 20 °C.min^{-1} from 20 to 580 °C. A test sample of 5-10 mg was used for each run (ASTM D2584).

2.3.5. Flame retardancy test

The flame retardancy test (LOI) was performed on the samples granule at the Giti Pasand Industrial Group laboratory under ISO/1EC 17025 terms.

2.3.6. Tensile properties

Mechanical properties are one of the most significant parameters in preparation of nanocomposites. The analysis of mechanical properties provides useful information about the effect of the compatibilizer, nanoclay, and process. The tensile strength tests and Young's modulus were performed in terms of ASTMD638 standards and 500 MPa.

2.3.7. Pipe Preparation

The sample of the pipe was prepared by extruder model Baufano (Italy): cylinder 200-220 °C, Head 210-220 °C, and Die 210-220 °C.

2.3.8. Ring stiffness

The ring stiffness test was carried out using the ISIR 111438 standard at 23 °C.

3. Results and discussion

3.1. SEM

The effect of the processing condition on the dispersion of the nanoclay in the PP matrix was studied using SEM (Fig. 1). The SEM results indicated that there is no particles agglomeration in EPD60R$_2$ and there is a satisfactory dispersion in the polymer matrix (Fig. 1(a)). Nanoclay particles are dispersed and agglomerated due to the high content of nanoclay. However, Fig. 1(b) shows that an increase of 5 wt% of nanoclay loading causes an agglomeration problem and non-uniform particle distribution of the C15A.

3.2. XRD

The XRD patterns of the nanoclay and nanocomposites are depicted in Fig. 2. The characteristic peak is observed at $2\theta = 7.19°$ in the nanoclay pattern. The D spacing of the nanoclay sheets, obtained using Bragg's equation ($n\lambda = 2d \sin\theta$), is 18.26A°. The angle of radiation for EPD60R$_1$ and nanocomposites EPD60R$_2$ and EPD60R$_3$ travels towards the fewer angle, which are $2\theta = 21.02°$, 6.55° and 6.28°, respectively. The peak point of the nanoparticles has a lower intensity and a higher band width in the nanocomposites. The *d*-spacing of
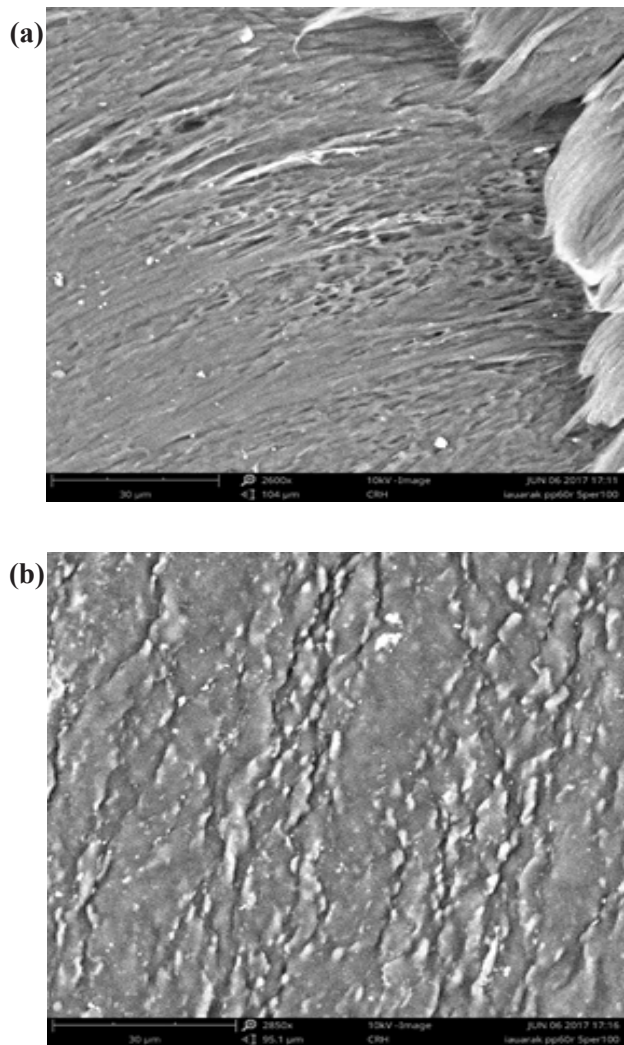
Fig. 1. SEM of (a) EPD60R$_2$ and (b) EPD60R$_3$.

EPD60R$_1$ and nanocomposites EPD60R$_2$ and EPD60R$_3$ are 6.27, 18.97, and 20.04A°, respectively. This indicates that enough polymer molecules enter between the nanoclay layers to affect higher intercalation and the polymeric chains penetrating into the interlayer spaces causes the nanoclay sheets separate from each other. Consequently, with an increase in interlayer distance, the peak point of the curve travels towards a lower 2θ and the amorphous materials do not form strong peaks. The qualitative analysis demonstrated that the crystals, which have an orderly structure, form certain peaks at certain angles (Fig. 2, Table 4).

3.3. DSC

The results of the DSC test is a curve of the heat flow ratio temperature and time. This can be in two states of exothermic and endothermic with a positive or negative peak. Then, the thermography of melting
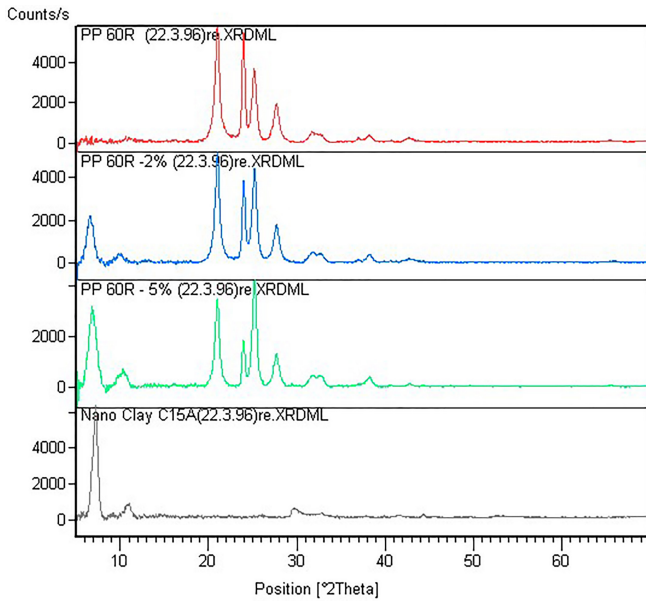
Fig. 2. XRD schematic graph for nanoclay, EPD60R$_1$, EPD60R$_2$ and EPD60R$_3$.

Table 4. XRD results for EPD60R$_1$, EPD60R$_2$, and EPD60R$_3$.

Batch No. ↓	2θ º	d (nm)
Nanoclay	7.19	18.26
EPD60R$_1$	21.02	6.27
EPD60R$_2$	6.553	18.97
EPD60R$_3$	6.228	20.04

and crystallization of heating and cooling processes was obtained, respectively. After that, the degree of crystallinity of the specimen was calculated using Eq. (1) [16,17].

$$X_C = [\Delta H_m / \Delta H_{100}] \times 100 \qquad (1)$$

In this equation, ΔH_{100} is the enthalpy of PP melting with a degree of crystallinity:

$$H_{100} = \Delta H_m \ (209 \ J/g)$$

Table 5 shows that EPD60R$_1$ has an initial crystallinity temperature (T_C) of 117.09 °C, That shift to the high temperature zone as a result of the combination of nanoclay, and also continuously increase as the nanoclay content is increased. The nanocomposites have an optimal T_C of 119.27 and 200.41 °C when containing 2 and 5 wt% nanoclay, respectively. Penetration of nanoclay into the polymer causes an increases in T_C. The melting temperature (T_m) consequently occurs in the crystallization phase in final hybrid product. The

Table 5. Crystallization of EPD60R$_1$, EPD60R$_2$, and EPD60R$_3$.

Batch No. ↓	T_C (ºC)	X_C (%)	T_m (ºC)
EPD60R$_1$	118.25	20.26	173.05
EPD60R$_2$	119.27	31.25	173.18
EPD60R$_3$	200.41	32.36	173.50

maximum crystallinity (X_C) is 32.36%. The degree of crystallinity for EPD60R$_2$ and EPD60R$_3$ increases about 54.24 and 59.23% compared to the EPD60R$_1$. This is due to the fact that nanoclay acts as a nucleating agent factor and increases the crystallization of EPD60R. Among the nucleates, nanoclay was found to be very efficient and its nucleation ability was also highly concentration dependent. In addition, it was shown that nucleation efficiency of a nucleate can be significantly increased by a new dispersion method comprised of solubilization in a microemulsion. Therefore, there is a significant relationship between crystallization and the percentage of nanoclay (Table 5).

3.4. TGA

The thermal stability of the nanocomposites was studied by the TGA technique. Fig. 3 shows the TGA thermographs of EPD60R/PP ternary nanocomposites with variable dosages of the compatibilizer. Thermographs reveal that the onset of degradation of the two nanocomposites shifts towards a higher temperature when the nanoclay concentration in the blend increases indicating higher thermal stability. The increased temperatures of nanocomposites samples in T^5 and T^{10} degradation compared to EPD60R$_1$ was also observed, this is attributed to the existence of nanoclay layers. The maximum degradation temperature also increased with compatiblizer loading. In fact, the
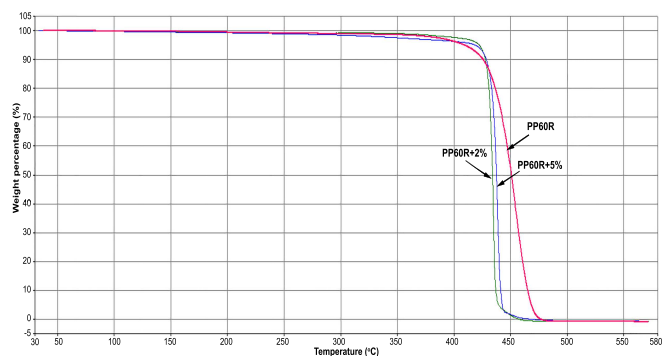

Fig. 3. TGA diagrams for EPD60R$_1$, EPD60R$_2$ and EPD60R$_3$.

intercalate structure of the nanocomposite reduced the transfer rate of volatile matters resulting in degradation from solid to gas phase and consequently increases the thermal stability. The residual weight also increased with nanoclay loading. The residual weight without nanoclay is 1.54% and increases with the incorporation of nanoclay to 2.17 and 5.08%, respectively (Fig. 3, Table 6).

Table 6. Thermal stability $EPD60R_1$, $EPD60R_2$ and $EPD60R_3$.

Batch No. ↓	T^5 (°C)	T^{10} (°C)	Residual weight (%)
$EPD60R_1$	415.5	425.3	1.54%
$EPD60R_2$	418.6	430.4	2.17%
$EPD60R_3$	425.2	436.7	5.08%

3.5. Flame retardancy

The main mechanism of flame retardancy for nanofillers involves the nanofiller acting as a barrier for gas flow and oxygen diffusion in the condensed phase. The flame retardancy test, which is based on the minimum amount of oxygen in the oxidation process, indicates the tendency of the polymer toward the burning process. The resistance against flame increases with the addition of nanoclay to the polymer matrix. By placing chains between the silicate sheets, the existence of pores in the nanoclay particles prevents produced gases escaping during the burning process. Therefore, more oxygen is required for burning. The $EPD60R_2$ and $EPD60R_3$ nanocomposites required 11.4 and 12.58% more oxygen to burn compared to $EPD60R_1$ (Table 7).

Table 7. Flame retardancy results of LOI for $EPD60R_1$, $EPD60R_2$ and $EPD60R_3$.

Batch No. ↓	$EPD60R_1$	$EPD60R_2$	$EPD60R_3$
LOI	27.5%	31.8%	34.6%

3.6. Tensile properties

Each specimen was measured three times and the mean values were represented. The diagrams of the Fig. 4 illustrate a reduction in tensile and an increase in Young's modulus indicating that nanoclay influences the ductility of $EPD60R_1$ and increase the tensile modulus. Adding the nanoclay not only improves the

connection at the joint surface between particles and background matter but also increases the number of hydrogenic interactions between the nanoclay and PP and consequently increases the tensile modulus. Tensile modulus was reported 274 and 321 MPa for $EPD60R_2$ and $EPD60R_3$ nanocomposites, respectively. These results indicate an increased tendency for the formation of amide bonds between ammonium nanoclay groups and MA groups and increases the MA ring opening reaction. Consequently, the tensile strength of the nanocomposites $EPD60R_2$ and $EPD60R_3$, compared to $EPD60R_1$ increases to 5 and 17%, respectively. And while adding nanoclay to PP and placing silicate layers between polymeric chains improves tensile modulus, it also reduces the viscosity property of the polymer. Therefore, elongation at break and elongation at yield were seen to be decreased. The elongation at break and elongation at yield points of nanocomposites $EPD60R_2$ and $EPD60R_3$ were decreased by 5, 11, and 0.9, 0.8%, respectively. The reduction of elongation at yield and at break may be due to greater interaction between the nanoclay and polymer matrix, which probably leads to a lower polymeric chain mobility making the materials more rigid (Fig. 4).
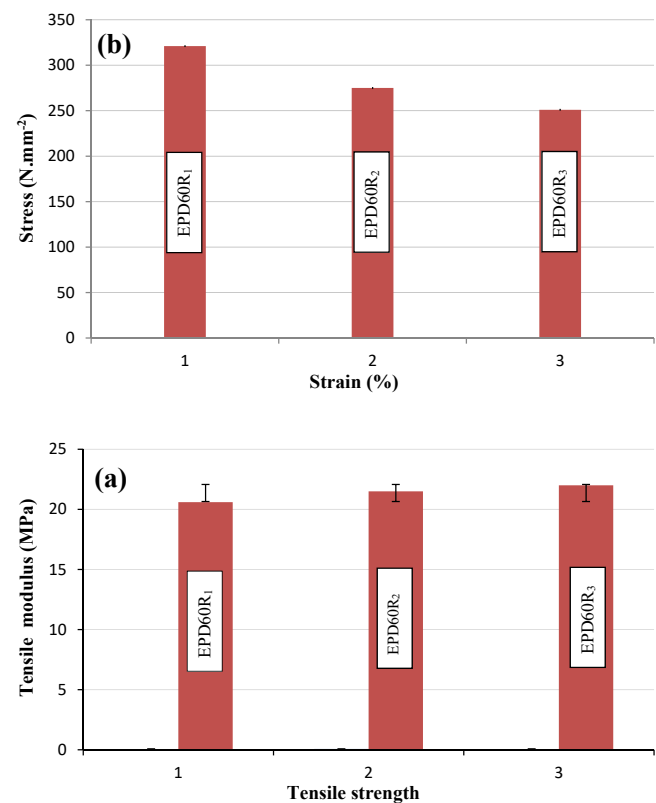

Fig. 4. (a) Tensile curve and (b) Stress-Strain curve of $EPD60R_1$, $EPD60R_2$, and $EPD60R_3$.

3.7. Flexural modulus

When the specimens are subjected to flexural strength tests, the compression tension and tensile tension are formed at the upper and lower surface of the specimen. Here (F), the maximum force, exerted on EPD60R$_1$ and the nanocomposites is different. The highest force exerted is attributed to nanocomposites EPD60R$_2$ and EPD60R$_3$.This represents an increase in nanoclay and (PP-*g*-MA) interaction. Indeed, high penetration of polymeric chains between silicate sheets results in a higher tensile strength for the nanocomposites. Consequently, the force of the flexural strength of the nanocomposites EPD60R$_2$ and EPD60R$_3$ increased up to 8 and 14 MPa respectively, compared to EPD60R$_1$ (Fig. 5, Table 8).

3.8. Ring stiffness test

Ring stiffness tests were performed on the prepared pipe from EPD60R$_1$ and EPD60R$_2$ a typically. As it can be seen in Table 9, EPD60R$_2$ ring stiffness rise by about 25% compared to EPD60R$_1$, which is the reason for the ring stiffness. Adding nanoclay increased crystallinity in the polymer because the nanoclay acts as a nucleated agent, based on DSC results stated in the preceding discussion (T_m, X_C); therefore, increasing the crystallinity enhances ring stiffness.
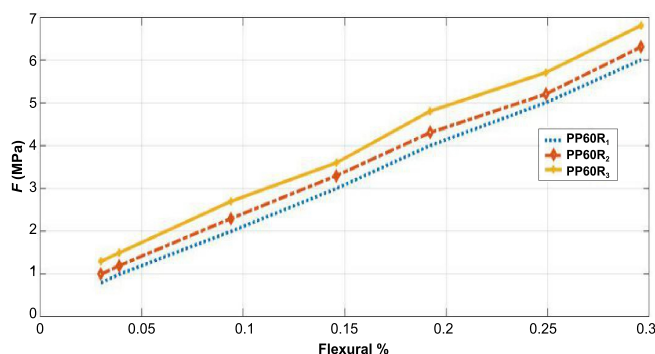

Fig. 5. Flexural strength diagram of EPD60R$_1$, EPD60R$_2$, and EPD60R$_3$.

Table 9. Ring stiffness results for EPD60R$_1$ and EPD60R$_2$.

Batch No. ↓	Ring stiffness(kN.m^{-2})	T (^{o}C)
EPD60R$_1$	3.8	23
EPD60R$_2$	4.75	23

4. Conclusion

In this study, we successfully prepared nanocomposites based on PP (EPD60R grade nanocomposites based on PP (EPD60R grade produced at the Shazand Petrochemical Company). The compatibility between the nanoclay and EPD60R matrix was significantly improved by the addition of maleic anhydride as a compatibilizer. The existence of a compatibilizer induced even more intercalation of the nanoclay. Nanoclay, (PP-*g*-MA) as compatibilizer, and polymer were combined using a melt mixing technology. Then, SEM, TGA, XRD, mechanical, and thermal tests were performed on the granule of specimens. The introduction of clay into the EPD60R matrix improved its properties. SEM imaging showed that the clay in the nanocomposites was dispersed uniformly in the EPD60R matrix. TGA studies revealed that the thermal stability of the nanocomposites improved in the presence of nanoclay. The XRD shows clay gallery separation or d-spacing increases at 2.5 wt% nanoclay, and thereafter remains unchanged so that nanocomposites form intercalated structure. However, the penetration of nanoparticles between the polymeric chains and increasing nanoclay content in the composite results in higher tensile modulus, crystallinity, LOI and thermal degradation temperatures. But it reduces the percentage of elongation at break and at the yield. Because non-pressure push fit pipe is used in underground applications, ring stiffness resistance is very important to inhibit deformation of the pipe. This research showed the addition of 2 wt% of nanoclay increased ring stiffness by 25%, but the impact strength of nanocomposite pipe was not obviously changed compared to pure polymer pipe.

Table 8. Flexural strength results for EPD60R$_1$, EPD60R$_2$, and EPD60R$_3$.

Batch No. ↓	EPD60R$_1$			EPD60R$_2$			EPD60R$_3$		
Points	1	2	3	1	2	3	1	2	3
Force (MPa)	1	2.5	4.9	1.25	3.1	5.3	1.56	3.5	5.6
Flexural	0.05	0.15	0.26	0.05	0.15	0.26	0.05	0.15	0.26

References

[1] A. Novruzova, M. Ramazanov, A. Chianese, F. Hajiyeva, A. Maharramov, U. Hasanova, Synthesis, structure and optical properties of PP+PbS/CdS hybrid nanocomposites, Chem. Engineer. Trans. 60 (2017) 61-66.

[2] L. Shen, F.Q. Wang, H. Yang, Q.R. Meng, The combined effects of carbon black and carbon fiber on the electrical properties of composites based on polyethylene or polyethylene/polypropylene blend, Polym. Test, 30 (2011) 442-448.

[3] M. Toyonaga, P.C. Kwan, M. Terano, T. Taniike, Well-defined polypropylene/polypropylene-grafted silica nanocomposites: Roles of number and molecular weight of grafted chains on mechanistic reinforcement, Polymers-Basel, 8 (2016) 300.

[4] C. Sharma, R. Dhiman, N. Rokana, H. Panwar, Nanotechnology: An untapped resource for food packaging, Front. Microbiol. 8 (2017) Article ID 1735.

[5] A. Buasri, N. Chaiyut, K. Borrornchettanwat, N. Chantanachi, K. Thanglor, Thermal and mechanical properties of modified CaCO₃/PP nanocomposites, Int. J. Chem. Mol. Nucl. Mater. Metall. Eng. 6 (2012) 689-692.

[6] A.B. Morgan, C.A. Wilkie, Flame Retardant Polymer Nanocomposites, John Wiley & Sons, New York, 2007.

[7] G. Smart, B.K. Candola, A.R. Horrocks, S. Nazaré, D. Marney, Polypropylene fibers coating dispersed clays having improved fire performance, Part II: Characterization of fibers and fabrics from PP-nanoclay blend, Polym. Advan. Technol. 19 (2008) 658-670.

[8] A.V. Rane, V.K. Abitha, Study of mechanical, thermal and micro structural properties of EPDM/ polypropylene/nanoclay composites with variable compatibilizer dosage, J. Mater. Environ. Sci. 6 (2015) 60-69.

[9] K. Ćwiek-Ludwicka, J.K. Ludwicki, Nanomaterials in food contact materials; considerations for risk assessment, Rocz. Panstw. Zakl. Hig. 68 (2017) 321-329.

[10] H.A. Patel, G.V. Joshi, R.R. Pawar, H.C. Bajaj, R.V. Jasra, Mechanical and thermal properties of polypropylene nanocomposite using organoclay, Polym. Composite. 31 (2010) 399-404.

[11] H. Plaza, R. Vergara, P. Zapata, Composites of polypropylene melt blended with synthesized silica nanoparticles, Compos. Sci. Technol. 71 (2011) 535-550.

[12] N.A. Rahman, A. Hassan, R. Yahya, R.A. Lafia-Araga, Glass fiber and nanoclay reinforced polypropylene composites morphological, thermal and mechanical Properties, Sains Malays. 42 (2013) 537-546.

[13] I. Dabrowska, L. Fambri, A. Pegotti, M. Slout, T. Vackova, J. Kolarik, Spinning, drawing and physical properties of propylene nanocomposite fibers with fumed nanosilica, Express Polym. Lett. 9 (2015) 277-290.

[14] J.Z. Zheng, X.P. Zhou, J.R. Ying, X.L. Xie, Y.W. Mai, Enhanced mechanical properties of polypropylene/silica nanocomposites with surface modification of nano-silica via *in-situ* copolymerization of methyl methacrylate and butyl acrylate, Chinese J. Polym. Sci. 27 (2009) 685-698.

[15] F. Mirjalili, L. Chuah, E. Salahi, Mechanical and morphological properties of polypropylene/nano α-Al₂O₃ composites, Sci. World J. 2014 (2014) Article ID 718765.

[16] G.S. Bhat, R.R. Hegde, M. G. Kamath, B. Deshpande, Nanoclay reinforced fibers and nonwovens, J. Eng. Fiber Fabr. 3 (2008) 22-34.

[17] M. Oda, Y. Tanabe, M. Noda, S. Inaba, E. Krayukhina, H. Fukada, S. Uchiyama, Structural and binding properties of laminarin revealed by analytical ultracentrifugation and calorimetric analyses, Carbohyd. Res. 431 (2016) 33-38.